Spectral Theory of the Turbulent Mean-Velocity Profile

Gustavo Gioia,[1] Nicholas Guttenberg,[2] Nigel Goldenfeld,[2] and Pinaki Chakraborty[3]
[1]Department of Mechanical Science and Engineering, University of Illinois, Urbana, Illinois 61801, USA
[2]Department of Physics, University of Illinois, Urbana, Illinois 61801, USA
[3]Department of Geology, University of Illinois, Urbana, Illinois 61801, USA
(Received 25 August 2009; published 25 October 2010)

It has long been surmised that the mean-velocity profile (MVP) of pipe flows is closely related to the spectrum of turbulent energy. Here we perform a spectral analysis to identify the eddies that dominate the production of shear stress via momentum transfer. This analysis allows us to express the MVP as a functional of the spectrum. Each part of the MVP relates to a specific spectral range: the buffer layer to the dissipative range, the log layer to the inertial range, and the wake to the energetic range. The parameters of the spectrum set the thickness of the viscous layer, the amplitude of the buffer layer, and the amplitude of the wake.

DOI: 10.1103/PhysRevLett.105.184501 PACS numbers: 47.27.N−, 47.27.Ak, 47.27.eb

Although most flows in nature and technology are turbulent flows over confining walls, these latter flows have remained amongst the less understood phenomena of classical physics [1]. Take the simplest example (an example whose applications are legion): the turbulent flow in a long smooth-walled pipe with a cross section of radius R. If the flux be kept steady, the velocity of the flow at a distance y from the wall of the pipe may be averaged over a long period of time to obtain a local mean velocity u. The function $u(y)$ is called the mean-velocity profile (MVP), and there is a MVP for each value of the Reynolds number, $\mathrm{Re} \equiv UR/\nu$, where U is the mean velocity of the flow (i.e., the flux divided by the cross-sectional area of the pipe) and ν is the kinematic viscosity of the fluid [2,3]. (Re quantifies the relative importance of inertia and viscosity in the flow; the higher the Re, the more turbulent the flow.) MVPs were first measured 80 years ago [4] and have recently been the subject of exacting experiments [5] and numerous computational simulations [6,7]. Theory has meanwhile lagged well behind experiments and simulations.

The first theory came soon after the earliest experiments. Ludwig Prandtl showed that when plotted in terms of the dimensionless "wall variables" $\tilde{u}$ and $\tilde{y}$, the MVPs for different values of Re collapse into a single MVP close to the wall (Fig. 1) [3]. The wall variables are defined by $\tilde{u} \equiv u/\sqrt{\tau_0/\rho}$ and $\tilde{y} \equiv y(\sqrt{\tau_0/\rho})/\nu$, where ρ is the density of the fluid and τ_0 is the shear stress—or shear force per unit area—that develops between the flow and the wall of the pipe. Prandtl also showed that over most of its domain $\tilde{u}(\tilde{y})$ follows the "log law of the wall,"

$$\tilde{u}(\tilde{y}) = \frac{1}{\kappa} \ln \tilde{y} + B, \tag{1}$$

where κ (the "Kármán constant") and B are dimensionless constants which can be estimated by fitting experimental data [3].

Numerous variants of the log law of the wall have been proposed, and recently it has been argued that the MVPs for different values of Re might not be logarithmic after all. Instead, they might be power laws with Re-dependent exponents and a logarithmic envelope [8]. Yet the original theory of Prandtl and this recent theory of Barenblatt have been predicated on dimensional analysis and similarity assumptions (they differ in the similarity assumptions [8]), without reference to the spectrum. As a result, these theories cannot be used to relate, for example, the log law of the wall or the constants thereof to the spectrum. Our aim here is to find the missing link between the MVP and the spectrum.

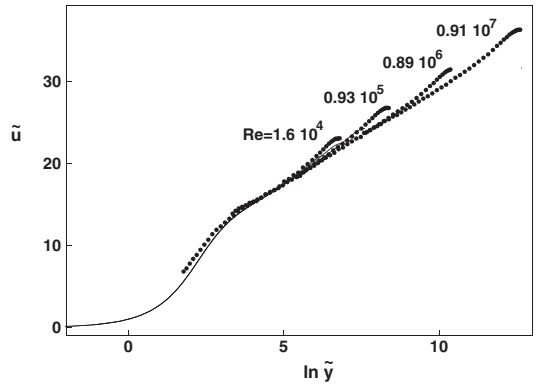

FIG. 1. Log-linear plots of the MVPs in the "wall variables" $\tilde{u}$ and $\tilde{y}$ for four values of Re. The symbols are from experiments [5] and the solid lines from simulations [7]. Each MVP extends from the wall (which corresponds always to $\tilde{y} = 0$) to the centerline of the pipe (which corresponds to a value of $\tilde{y}$ that depends on Re); the MVPs collapse on a single MVP close to the wall. Focusing on any one MVP, we can parse the horizontal axis from left to right to find the "viscous layer" (where the MVP has a positive curvature), the "buffer layer" (where the MVP has a noticeable negative curvature), the "log layer" [where the MVP follows the log law of the wall (1)], and a "wake" (where the MVP overshoots the log law of the wall close to the centerline of the pipe) [18].

We adopt the imagery of "turbulent eddies" [9,10] and use the spectrum of turbulent energy [2,11], $E(k) \equiv \frac{2}{3} \times (\kappa_\varepsilon \varepsilon)^{2/3} k^{-5/3} c_d(\eta k) c_e(Rk)$, to determine the velocity of the eddies of size s, v_s, in the form $v_s^2 = \int_{1/s}^{\infty} E(k)dk$. Here k is the wave number, κ_ε is a dimensionless parameter, ε is the turbulent power per unit mass [12], $\eta = \nu^{3/4}\varepsilon^{-1/4}$ is the viscous length scale [2], R is the largest length scale in the flow, $\frac{2}{3}(\kappa_\varepsilon \varepsilon)^{2/3} k^{-5/3}$ is the Kolmogorov spectrum [13,14], and c_d and c_e are dimensionless correction functions—the dissipative-range correction and the energetic-range correction, respectively. For the dissipative-range correction we adopt the usual form, $c_d(\eta k) = \exp(-\beta_d \eta k)$, and for the energetic-range correction the form proposed by Kármán, $c_e(Rk) = (1 + (\beta_e/Rk)^2)^{-17/6}$, where β_d and β_e are nonnegative dimensionless parameters [11]. Note for future reference that as $v_s^2 = \int_{1/s}^{\infty} E(k)dk$ and $E(k) \geq 0$ for all k, the velocity of an eddy increases with the size of the eddy.

By introducing the dimensionless variable $\xi \equiv sk$, we can write $v_s = (\kappa_\varepsilon \varepsilon s)^{1/3}\sqrt{I}$, where $I \equiv \mathcal{I}(\eta/s, s/R) \equiv \frac{2}{3}\int_1^{\infty} \xi^{-5/3} \exp(-\xi\beta_d \eta/s)(1 + (\beta_e s/R)^2/\xi^2)^{-17/6} d\xi$. For s in the inertial range ($\eta \ll s \ll R$), $I = 1$, and therefore $v_s = (\kappa_\varepsilon \varepsilon s)^{1/3}$ [2,10,11], which is the well-known expression for the velocity of an eddy of the inertial range (i.e., an eddy of size $\eta \ll s \ll R$). The same expression may be independently derived from Kolmogórov's four-fifth law, which also gives the convenient estimate $\kappa_\varepsilon = 4/5$ [15]. For s outside of the inertial range, $I < 1$. It follows that an eddy of the dissipative range or the energetic range (i.e., an eddy of size $s \approx \eta$ or $s \approx R$, respectively) has a velocity $v_s < (\kappa_\varepsilon \varepsilon s)^{1/3}$—i.e., the eddy is *slower* than an imaginary eddy of the same size in the inertial range.

We now seek to derive an expression for the turbulent shear stress τ_t in a smooth-walled pipe of radius R. Let us call W_y the wetted surface at a distance y from the wall (Fig. 2). The turbulent shear stress that acts on W_y is produced by eddies that straddle W_y and transfer momentum across W_y (Fig. 2). Thus an eddy of size s carries fluid of high horizontal momentum per unit volume [about $\rho u(y + s)$] downward across W_y and fluid of low horizontal momentum per unit volume [about $\rho u(y - s)$] upwards across W_y, and the eddy spans a momentum contrast $\rho(u(y + s) - u(y - s)) \approx 2\rho s u'(y)$ [16], where $u' \equiv du/dy$. The rate of momentum transfer across W_y is set by the velocity normal to W_y, i.e., the velocity of the eddy, v_s. Therefore, the turbulent shear stress produced by an eddy of size s scales as $\rho s u'(y) v_s$ (the product of the momentum contrast times the rate of momentum transfer).

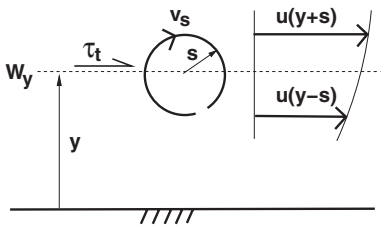

FIG. 2. Schematic for the derivation of the turbulent shear stress. $u(y + s)$ is the mean velocity at a distance $y + s$ from the wall; $u(y - s)$ is the mean velocity at a distance $y - s$ from the wall.

In order to identify the *dominant* eddies that straddle W_y, recall that v_s (and therefore sv_s) increases with s. It follows that the larger the eddy the larger the turbulent shear stress produced by the eddy. Nonetheless, eddies much larger than y do not properly straddle W_y and can provide only a negligible velocity normal to W_y, and therefore a negligible turbulent shear stress. (This observation is purely a matter of geometry.) We conclude that the dominant eddies that straddle W_y are the eddies of size $s = y$. The turbulent shear stress at a distance y from the wall is thus given by the expression, $\tau_t = \kappa_\tau \rho y v_y u'(y)$, where κ_τ is a dimensionless proportionality constant. From $\tau_t = \kappa_\tau \rho y v_y u'(y)$, $v_y = (\kappa_\varepsilon \varepsilon y)^{1/3}\sqrt{I}$, and $\varepsilon = \tau_t u'/\rho$ (the energy equation [11]), we can eliminate v_y and ε to obtain

$$\tau_t = \kappa^2 \rho I^{3/4} y^2 u'(y)^2, \tag{2}$$

where $\kappa \equiv (\kappa_\varepsilon \kappa_\tau^3)^{1/4}$.

Now, the total shear stress at a distance y from the wall is $\tau_0(1 - y/R)$, where τ_0 is the shear stress at the wall [11]. To obtain an equation for the MVP, we substitute (2) in the equation, $\tau_t + \rho\nu u' = \tau_0(1 - y/R)$, where $\rho\nu u'$ is the viscous shear stress, and rewrite the result in terms the Reynolds number $\mathrm{Re} \equiv UR/\nu$, the friction factor $f \equiv \tau_0/\rho U^2$, and the dimensionless variables $\hat{y} \equiv y/R$ and $\hat{u} \equiv u/U$:

$$\kappa^2 I^{3/4} \hat{y}^2 \hat{u}'^2 + \mathrm{Re}^{-1}\hat{u}' - f(1 - \hat{y}) = 0, \tag{3}$$

where $\hat{u}' \equiv d\hat{u}/d\hat{y}$ and $I \equiv \mathcal{I}(\eta/y, \hat{y})$. To obtain an equation for η/y, we substitute the energy equation, $\varepsilon = (fU^2(1 - y/R) - \nu u')u'$, into $\eta = \nu^{3/4}\varepsilon^{-1/4}$, and change variables to $\hat{y}$ and $\hat{u}$:

$$\eta/y = \mathrm{Re}^{-1/2}(f\mathrm{Re}\hat{u}'(1 - \hat{y}) - \hat{u}'^2)^{-1/4}\hat{y}^{-1}. \tag{4}$$

If for a fixed Re we let $\hat{y} \to 0$, then $\eta/y \to \infty$ [from (4)], $I \to \mathcal{I}(\infty, \hat{y}) = 0$, and (3) simplifies to $\hat{u}' = f\mathrm{Re}$, which is the law of the viscous layer. If for a fixed $\hat{y} \ll 1$ we let $\mathrm{Re} \to \infty$, then $\eta/y \to 0$ [from (4)], y is in the inertial range (where $I = 1$), and (3) simplifies to $\hat{u}' = \sqrt{f}/\kappa\hat{y}$, which we recognize as the log law of the wall with a Kármán constant $\kappa = (\kappa_\varepsilon \kappa_\tau^3)^{1/4}$. Note that the log law of the wall prevails where y is in the inertial range; it follows that the dominant eddies in the log layer are eddies of the inertial range. The presence of κ_ε and κ_τ in the expression for κ reminds us of the underpinnings of the theory: the spectrum and the momentum transfer, respectively. From $\kappa_\varepsilon = 4/5$ (the estimate from Kolmogórov's four-fifth law [15,17]) and $\kappa = 0.42$ (the experimental value [5]), we can estimate $\kappa_\tau = 0.34$.

The law of the viscous layer and the log law of the wall may be made invariant to changes in Re and f, in the form $\tilde{u}' = 1$ and $\tilde{u}' = 1/\kappa\tilde{y}$, by choosing $\tilde{y} \equiv \mathrm{Re}\sqrt{f}\hat{y} = \mathrm{Re}\sqrt{f}y/R$ and $\tilde{u} \equiv \hat{u}/\sqrt{f} = u/U\sqrt{f}$, which we recognize as the wall variables. In the wall variables (3) becomes

$$\kappa^2 I^{3/4} \tilde{y}^2 \tilde{u}'^2 + \tilde{u}' - (1 - \tilde{y}/\mathrm{Re}\sqrt{f}) = 0, \quad (5)$$

where $I \equiv \mathcal{I}(\eta/y, \tilde{y}/\mathrm{Re}\sqrt{f})$, and (4) becomes

$$\eta/y = (\tilde{u}'(1 - \tilde{y}/\mathrm{Re}\sqrt{f}) - \tilde{u}'^2)^{-1/4} \tilde{y}^{-1}. \quad (6)$$

From these equations it is apparent that in the wall variables there is a single MVP except close to the centerline of the pipe, where $\tilde{y} \approx \mathrm{Re}\sqrt{f}$ (or $y \approx R$).

We now ascertain under what conditions (5) and (6) are compatible with a nonvanishing turbulent shear stress close to the wall. Suppose that at a point $\tilde{y} \ll \mathrm{Re}\sqrt{f}$ (or $y \ll R$) we have $I = \mathcal{I}(\eta/y, 0) > 0$, and therefore $\tau_t > 0$. Then, we can eliminate $\tilde{u}'$ from (5) and (6) to obtain

$$\tilde{y} = \left(\frac{(\eta/y)^{4/3} + \kappa^{4/3} \mathcal{I}^{1/2}(\eta/y, 0)}{\kappa^{2/3} (\eta/y)^{8/3} \mathcal{I}^{1/4}(\eta/y, 0)} \right)^{1/2}. \quad (7)$$

Plots of $\tilde{y}$ vs η/y [Fig. 3(a)] reveal that for any given κ and β_d there exists a minimum value of $\tilde{y}$, to be denoted $\tilde{y}_v$. Therefore, for $\tilde{y} < \tilde{y}_v$ it must be that $I = 0$, $\tau_t = 0$, and $\tilde{u}' = 1$. As this latter equation is the law of the viscous layer, we identify $\tilde{y}_v$ with the thickness of the viscous layer [18]. Note that $\tilde{y}_v$ depends on the dissipative-range parameter β_d [Fig. 3(b)], and that for $\beta_d = 0$ there is no viscous layer ($\tilde{y}_v = 0$).

We are now ready to compute the MVP. For simplicity we use the Blasius relation for the friction factor, $f = 0.033\mathrm{Re}^{-1/4}$ [5]. For the spectral parameters β_d and β_e we use the values, $\beta_d = 7$ and $\beta_e = 8$. The thickness of the viscous layer is set by β_d and κ; for $\beta_d = 7$ and $\kappa = 0.42$, $\tilde{y}_v = 4.17$ [Fig. 3(b)]. Therefore, for $\tilde{y} < 4.17$ we can write $\tilde{u}(\tilde{y}) = \tilde{y}$, and for $\tilde{y} > 4.17$ we must compute $\tilde{u}(\tilde{y})$ by integrating (5) with boundary condition $\tilde{u}(4.17) = 4.17$. The results are shown in Fig. 4(a). Given the spectrum, the theory yields the entire MVP with all of its distinctive features. The specific connection between each one of these features and the spectrum will become apparent in what follows.

To elucidate the effect of the energetic-range correction, we recompute the MVP using $\beta_e = 10$ (a larger value than before) and $\beta_e = 0$ (the smallest possible value, which corresponds to having no energetic-range correction). The results [Fig. 4(b)] indicate that the energetic-range correction steepens the MVP in the wake. The dominant eddies in the wake must therefore be eddies of the energetic range. These eddies are slowed down by the energetic-range correction (and made less adept at transferring momentum). This effect explains the steepening of the MVP in the wake.

We have seen that the dissipative-range correction sets the thickness of the viscous layer [Fig. 3(b)]. To understand further the effects of the dissipative-range correction, we recompute the MVP using a few values of β_d, including $\beta_d = 0$ (the smallest possible value, which corresponds to having no dissipative-range correction). The results [Fig. 4(c)] indicate that the dissipative-range correction causes the buffer layer to form, so that for $\beta_d = 0$ there is no buffer layer. (The buffer layer is the part of the MVP where the MVP has a negative curvature [18].) The dominant eddies in the buffer layer must therefore be eddies of the dissipative range. These eddies are slowed down by the dissipative-range correction; the larger the eddies, the less they are slowed down, and the more adept they remain at transferring momentum. As the size of the dominant eddies increases with the distance to the wall, the MVP becomes less steep as we traverse the buffer layer from the outer edge of the viscous layer (where the eddies are fully viscous) to the inner edge of the log layer (where the eddies are fully inertial). This effect explains the negative curvature of the MVP in the buffer layer.

It is apparent from Fig. 4(c) that the constant B of the log law of the wall is set by β_d. A plot of B as a function of β_d is shown in Fig. 4(d).

Interestingly, the MVP for $\beta_d = 0$ can be obtained analytically everywhere save the wake. In fact, for $\beta_d = 0$ and $\tilde{y} \ll \mathrm{Re}\sqrt{f}$ (or $y \ll R$), $I = 1$ and (5) simplifies to $\kappa^2 \tilde{y}^2 \tilde{u}'^2 + \tilde{u}' - 1 = 0$, which with $\tilde{u}(0) = 0$ yields

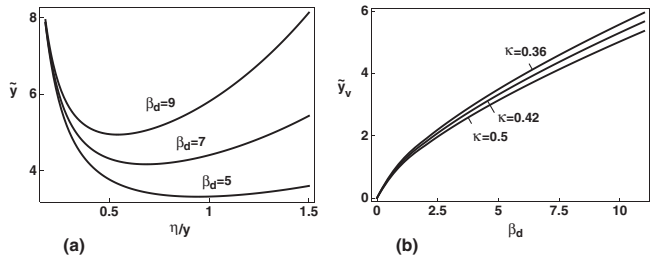

FIG. 3. (a) Plots of (7) for $\kappa = 0.42$ and three values of β_d. (b) Plots of the thickness of the viscous layer $\tilde{y}_v$ as a function of β_d for three values of κ.

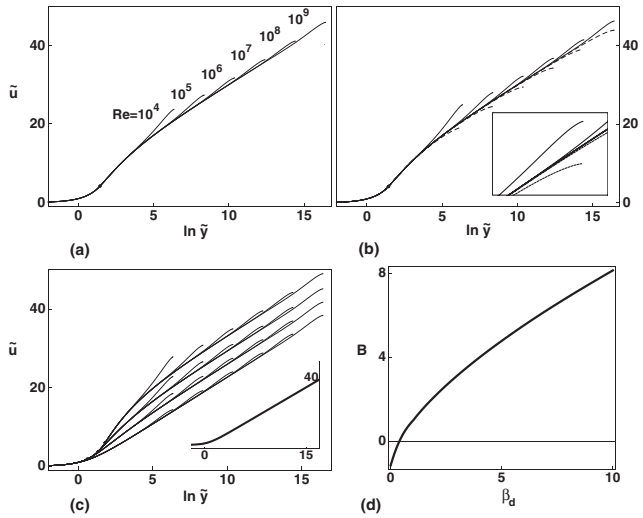

FIG. 4. (a) The MVPs computed using $\kappa = 0.42$, $\beta_e = 7$, and $\beta_d = 8$. The thick dot indicates the point of contact between the viscous layer and the buffer layer. (b) The same as in (a) but using $\beta_e = 0$ (dashed lines) and $\beta_e = 10$ (solid lines). Inset: detail of the wakes. (c) The same as in (a) but using $\beta_d = 0$ (bottom), 2, 6, and 12 (top). Inset: A plot of (8) for $\kappa = 0.42$. (d) A plot of B as a function β_d for $\kappa = 0.42$.

$$\tilde{u} = \frac{\operatorname{arcsinh}(2\kappa\tilde{y})}{\kappa} + \frac{1 - \sqrt{1 + \kappa^2\tilde{y}^2}}{2\kappa^2\tilde{y}}. \quad (8)$$

This is what the MVP would be away from the wake if the Kolmogorov spectrum were valid even for vanishingly small eddies [inset of Fig. 4(c)]. For $0 \ll \tilde{y} \ll \mathrm{Re}\sqrt{f}$ (or $0 \ll y \ll R$), (8) simplifies asymptotically to $\tilde{u} \sim (1/\kappa)\ln\tilde{y} + B$, with $B = (-1 + \ln 4\kappa)/\kappa$. Thus, for $\beta_d = 0$ and $\kappa = 0.42$, $B = -1.15$ in accord with Fig. 4(d).

We have established the long-surmised link [2] between the mean-velocity profile and the turbulent spectrum. To test our results, we have shown that the usual model of the spectrum (a power-law inertial range with corrections for the dissipative range and the energetic range) is in itself sufficient to compute with no additional assumptions a mean-velocity profile complete with viscous layer, buffer layer, log layer, and wake [19]. The thickness of the viscous layer, the two constants of the log law of the wall, and the amplitude of the wake are all set by the dimensionless momentum-transfer constant κ_τ and the usual spectral parameters—the parameter β_e of the energetic-range correction and the parameter β_d of the dissipative-range correction. The relation between a specific feature of the MVP and the spectral parameters reminds us of the underlying physics. Thus, for example, the Kármán constant is independent of both β_e and β_d, and is therefore unaffected by the energetic-range and dissipative-range corrections, with the implication that the eddies that dominate the momentum transfer in the log layer are eddies of the inertial range. More broadly, the close relation between the mean-velocity profile and the spectrum indicates that in turbulence, as in continuous phase transitions, global variables are governed by the statistics of the fluctuations [20].

This work was funded by NSF through grant DMR06–04435. P. C. acknowledges financial support from the Roscoe G. Jackson II Research Fellowship and the Charles R. Walgeen Jr. Chair funds. We have benefited from discussions with Carlo Zuñiga Zamalloa.

[1] B. Hof *et al.*, Science **305**, 1594 (2004); V. S. L'vov, I. Procaccia, and O. Rudenko, Phys. Rev. Lett. **100**, 054504 (2008).

[2] H. Tennekes and J. L. Lumley, *A First Course in Turbulence* (MIT Press, Cambridge, MA, and London, 1972).

[3] L. Prandtl, *Essentials of Fluid Dynamics* (Blackie & Son, London, 1953), 3rd ed., Chap. III.

[4] Reprinted in English in J. Nikuradse, *National Advisory Committee for Aeronautics Technical Memorandum* 1292 (Washington, D.C., 1950).

[5] M. V. Zagarola and A. J. Smits, J. Fluid Mech. **373**, 33 (1998); B. J. McKeon *et al.*, *ibid.* **501**, 135 (2004).

[6] J. G. M. Eggels *et al.*, J. Fluid Mech. **268**, 175 (1994); J. M. J. den Toonder and F. T. M. Nieuwstadt, Phys. Fluids **9**, 3398 (1997).

[7] S. Hoyas and J. Jimenez, Phys. Fluids **18**, 011702 (2006); J. C. del Alamo *et al.*, J. Fluid Mech. **500**, 135 (2004).

[8] G. I. Barenblatt, J. Fluid Mech. **248**, 513 (1993); G. I. Barenblatt and A. J. Chorin, Proc. Natl. Acad. Sci. U.S.A. **101**, 15 023 (2004).

[9] L. F. Richardson, Proc. R. Soc. A **110**, 709 (1926).

[10] U. Frisch, *Turbulence* (Cambridge University Press, Cambridge, England, 1995).

[11] S. B. Pope, *Turbulent Flows* (Cambridge University Press, Cambridge, England, 2000).

[12] G. I. Taylor, Proc. R. Soc. A **151**, 421 (1935); D. Lohse, Phys. Rev. Lett. **73**, 3223 (1994); Ch. R. Doering and P. Constantin, *ibid.* **69**, 1648 (1992).

[13] Reprinted in English in A. N. Kolmogórov, Proc. R. Soc. A **434**, 9 (1991).

[14] On the Kolmogórov spectrum and anisotropy, see B. Knight and L. Sirovich, Phys. Rev. Lett. **65**, 1356 (1990); T. S. Lundgren, Phys. Fluids **14**, 638 (2002); T. S. Lundgren, *ibid.* **15**, 1074 (2003); The view of anisotropy as a perturbation superposed on the isotropic flow [see, e.g., L. Biferale and I. Procaccia, Phys. Rep. **414**, 43 (2005)] might break down close to a wall, where the exponents themselves might change, albeit slightly [see C. M. Casciola, P. Gualtieri, B. Jacob, and R. Piva, Phys. Rev. Lett. **95**, 024503 (2005)].

[15] The four-fifth law reads $\bar{u}_s^3 = -(4/5)\varepsilon s$, where the left-hand side is the third-order structure function. The estimate $|\bar{u}_s^3| = v_s^3$ leads to $\varepsilon = (5/4)v_s^3/s$, or $\kappa_\varepsilon = 4/5$.

[16] We retain only the 1st term of the Taylor series because (a) additional terms would necessitate BCs other than the no-slip BC and (b) in our final solution for $u(y)$ the 2nd term $\leq 11\%$ of the 1st term for all y.

[17] Experimental and computational estimates of κ_ε are invariably of O(1) but differ slightly for different types of flow; K. R. Sreenivasan, Phys. Fluids **10**, 528 (1998). The implication here is that the Kármán constant may depend mildly on the type of flow.

[18] We define the viscous layer, the buffer layer, etc., (caption of Fig. 1), as in Chap. 5 of [2], in particular, Fig. 5.6.

[19] Models of the spectrum that retain a dependence on Re in the inertial range [see, e.g., G. I. Barenblatt and N. Goldenfeld, Phys. Fluids **7**, 3078 (1995)] may lead to alternative MVPs with a Re-dependent power-law layers (see [8]) instead of a log layer, and may help explain the Reynolds-number effects that have been measured in the overlap region [see, e.g., M. Gad-el-Hak and P. R. Bandyopahyay, Appl. Mech. Rev. **47**, 307 (1994); A. Praskovsky and S. Oncley, Phys. Fluids **6**, 2886 (1994); Y. Tsuji, J. H. M. Fransson, P. H. Alfredsson, and A. V. Johansson, J. Fluid Mech. **585**, 1 (2007)].

[20] G. Gioia and F. A. Bombardelli, Phys. Rev. Lett. **88**, 014501 (2001); G. Gioia and P. Chakraborty, *ibid.* **96**, 044502 (2006); G. Gioia and F. Bombardelli, *ibid.* **95**, 014501 (2005); N. Goldenfeld, *ibid.* **96**, 044503 (2006); G. Gioia, P. Chakraborty, and F. A. Bombardelli, Phys. Fluids **18**, 038107 (2006); M. Mehrafarin and N. Pourtolami, Phys. Rev. E **77**, 055304(R) (2008); N. Guttenberg and N. Goldenfeld, *ibid.* **79**, 065306(R) (2009); E. Calzetta, *ibid.* **79**, 056311 (2009).